Atomic Carbon as a Terminal Ligand: Studies of a Carbidomolybdenum Anion Featuring Solid-State ^{13}C NMR Data and Proton-Transfer Self-Exchange Kinetics

Jane B. Greco,[†] Jonas C. Peters,[†,§] Thomas A. Baker,[†] William M. Davis,[†] Christopher C. Cummins,*[,†] and Gang Wu*[,‡]

Contribution from the Departments of Chemistry, Massachusetts Institute of Technology, 77 Massachusetts Ave., Cambridge, Massachusetts 02139-4307, and Queen's University, Kingston, Ontario, Canada K7L 3N6

Received September 29, 2000

Abstract: Anion $[CMo(N[R]Ar)_3]^-$ (R = $C(CD_3)_2CH_3$ or ^{t}Bu, Ar = 3,5-$C_6H_3Me_2$) containing one-coordinate carbon as a terminal substituent and related molecules have been studied by single-crystal X-ray crystallography, solution and solid-state ^{13}C NMR spectroscopy, and density functional theory (DFT) calculations. Chemical reactivity patterns for $[CMo(N[R]Ar)_3]^-$ have been investigated, including the kinetics of proton-transfer self-exchange involving $HCMo(N[R]Ar)_3$, the carbidomolybdenum anion's conjugate acid. While the Mo≡C bond lengths in $[K(benzo\text{-}15\text{-}crown\text{-}5)_2][CMo(N[R]Ar)_3]$ and the parent methylidyne, $HCMo(N[R]Ar)_3$, are statistically identical, the carbide chemical shift of δ 501 ppm is much larger than the δ 282 ppm shift for the methylidyne. Solid-state ^{13}C NMR studies show the carbide to have a much larger chemical shift anisotropy (CSA, 806 ppm) and smaller $^{95}Mo-^{13}C$ coupling constant (60 Hz) than the methylidyne (CSA = 447 ppm, $^1J_{MoC}$ = 130 Hz). DFT calculations on model compounds indicate also that there is an increasing MoC overlap population on going from the methylidyne to the terminal carbide. The pK_a of methylidyne $HCMo(N[R]Ar)_3$ is approximately 30 in THF solution. Methylidyne $HCMo(N[R]Ar)_3$ and carbide $[CMo(N[R]Ar)_3]^-$ undergo extremely rapid proton-transfer self-exchange reactions in THF, with $k = 7 \times 10^6$ M^{-1} s^{-1}. Besides being a strong reducing agent, carbide $[CMo(N[R]Ar)_3]^-$ reacts as a nucleophile with elemental chalcogens to form carbon−chalcogen bonds and likewise reacts with PCl_3 to furnish a carbon−phosphorus bond.

1. Introduction

Small-molecule reductive cleavage reactions mediated by the three-coordinate molybdenum(III) complex $Mo(N[R]Ar)_3$ (**1**, R = $C(CD_3)_2CH_3$ or ^{t}Bu, Ar = 3,5-$C_6H_3Me_2$) have opened new pathways for the synthesis of molybdenum−element multiple bonds.[1,2] A highlight in this regard has been the preparation and structural characterization of a carbidomolybdenum(VI) anion, in which the terminal carbide (formally C^{4-}) ligand is derived from carbon monoxide.[3] The anion, $[CMo(N[R]Ar)_3]^-$ ($[\mathbf{1\text{-}C}]^-$), is an exotic example of one-coordinate carbon bonded solely to a transition metal center; other examples of molecules containing one-coordinate carbon are organic isonitriles, cyanide, and carbon monoxide. In addition, Templeton and co-workers have described a carbidotungsten(IV) anion.[4]

In the course of converting monocarbonyl **1-CO** to salts of the title carbidomolybdenum anion $[\mathbf{1\text{-}C}]^-$ several molecules were obtained as depicted in Scheme 1, noteworthy among which are **1-CH** and **1-COC(O)^{t}Bu**. These molecules are found to be of interest with respect to their physical properties, such as NMR parameters, parameters discussed here in comparison with those for $[\mathbf{1\text{-}C}]^-$. Three Mo−C coupling constants ($^1J_{MoC}$) have been determined, and these are correlated to ^{13}C chemical shift and bonding parameters. Physical methods used to probe these molecules include single-crystal X-ray diffraction and solution- and solid-state ^{13}C NMR spectroscopies, while density functional theory (DFT) calculations have been used to provide insight into the bonding.

Herein it is shown that the rate of degenerate proton transfer between $[\mathbf{1\text{-}C}]^-$ and its conjugate acid, the methylidyne $HCMo(N[R]Ar)_3$ **(1-CH)**, is very fast, an observation noteworthy in that fast proton exchange rates are unusual for carbanions.[5] In addition to proton exchange rate studies, the pK_a of the methylidyne **1-CH** has been determined, and nucleophilic patterns of reactivity have been established for the anion $[\mathbf{1\text{-}C}]^-$.

This work enhances the literature concerning CO-derived transition metal carbido complexes.[6−9] Chisholm has reported the formation of a μ_4-carbide from $W_4(OCH_2\text{-}c\text{-}Pen)_{12}$ and CO,[10] while Wolczanski showed that CO reacts with $Ta(silox)_3$ (silox = ^{t}Bu_3SiO) to form a dinuclear bridging dicarbide and with $[WCl(silox)_2]_2$ to form a dinuclear monocarbide-bridged species.[11,12] Recently, Floriani has communicated the stepwise

[†] Massachusetts Institute of Technology.
[‡] Queen's University.
[§] Current address: California Institute of Technology.

(1) Cummins, C. C. *Prog. Inorg. Chem.* **1998**, *47*, 685.
(2) Cummins, C. C. *J. Chem. Soc., Chem. Commun.* **1998**, 1777.
(3) Peters, J. C.; Odom, A. L.; Cummins, C. C. *J. Chem. Soc., Chem. Commun.* **1997**, 1995.
(4) Templeton, J. L.; et al. *J. Am. Chem. Soc.* **2001**, *123*, 4992−5002.
(5) Kresge, A. J. *Acc. Chem. Res.* **1975**, *8*, 354.
(6) Mansuy, D.; Lecomte, J.-P.; Chottard, J.-C.; Bartoli, J.-F. *Inorg. Chem.* **1980**, *20*, 3119.
(7) Etienne, M.; White, P. S.; Templeton, J. L. *J. Am. Chem. Soc.* **1991**, *113*, 2324.
(8) Latesky, S. L.; Selegue, J. P. *J. Am. Chem. Soc.* **1987**, *109*, 4731.
(9) Casselli, A.; Solari, E.; Scopelliti, R.; Floriani, C. *J. Am. Chem. Soc.* **2000**, *122*, 538.
(10) Chisholm, M. H.; Hammond, C. E.; Johnston, V. J.; Streib, W. E.; Huffman, J. C. *J. Am. Chem. Soc.* **1992**, *114*, 7056.

10.1021/ja003548e CCC: $20.00
Published on Web 05/04/2001

Scheme 1

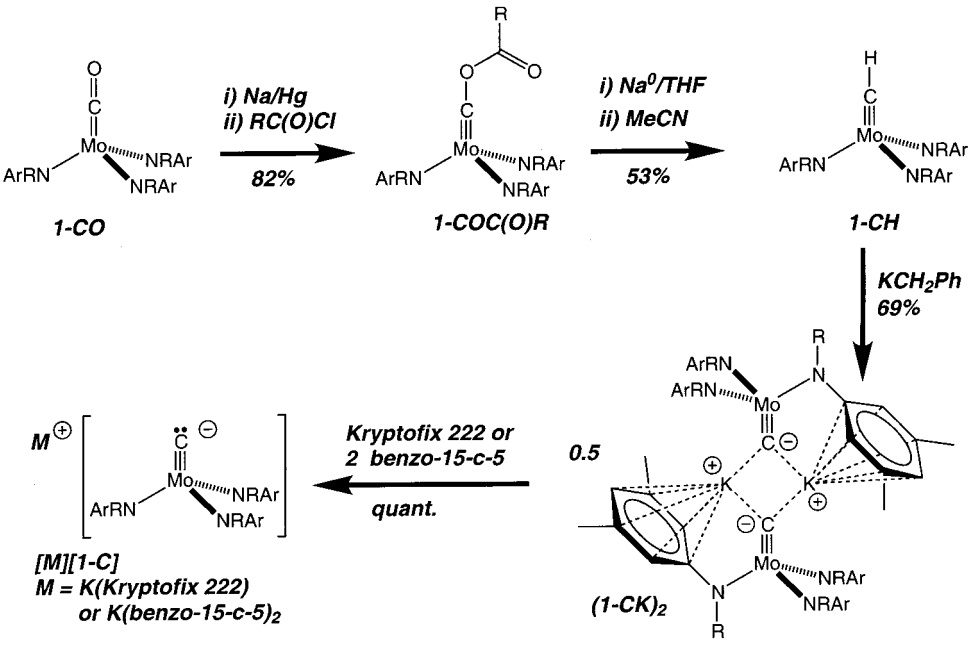

scission of CO by a niobium−calixarene dimer to produce a diniobium μ-carbide complex.[9]

2. Results and Discussion

1. Preparation of [1-^{13}C]$^-$. The preparation of [**1**-^{13}**C**]$^-$ or its natural abundance isotopomer consists of a multistep synthesis (Scheme 1) in which an oxygen atom is removed from carbonyl **1**-^{13}**CO** or **1-CO**. Reduction of **1**-^{13}**CO** with Na/Hg, followed by quenching with pivaloyl chloride, yielded **1**-^{13}**COC(O)^{t}Bu** in 82% yield. The latter pivalatocarbyne was subsequently reduced with sodium metal in THF, and the mixture was quenched with acetonitrile to yield **1**-^{13}**CH**, which could be deprotonated with benzyl potassium (KBn) to produce (**1**-^{13}**CK**)$_2$. Formulation of the latter as a dimer incorporating a K_2C_2 square core and intramolecular alkali metal−aryl interactions is based upon analogy with the closely related, structurally characterized nitridoniobium derivative {(Ar[R]N)$_3$Nb-NNa}$_2$,[13] in addition to information gleaned from a preliminary X-ray diffraction study on (**1**-^{13}**CK**)$_2$ itself.[14] The ion-separated salts [K(Kryptofix 222)][**1**-^{13}**C**] and [K(benzo-15-crown-5)$_2$][**1**-^{13}**C**] were easily prepared by addition of 1 equiv of Kryptofix 222 or 2 equiv of benzo-15-crown-5, respectively, to 0.5 equiv of potassium derivative (**1**-^{13}**CK**)$_2$.

2. Molecular Structure of Methylidyne 1-CH. A single-crystal X-ray diffraction study of **1-CH** was undertaken for comparison with the previously reported structure of [K(benzo-15-crown-5)$_2$][**1-C**].[3] A thermal ellipsoid plot of the structure of **1-CH** is shown in Figure 1. The Mo≡C bond length of 1.702(5) Å is statistically identical to the Mo≡C bond length of 1.713(9) Å for [K(benzo-15-crown-5)$_2$][**1-C**]. There is little difference in the Mo−N bond lengths between the two structures: 1.964(4), 1.981(4), and 1.991(4) Å for **1-CH** compared with 2.008(6), 2.010(7), and 2.013(6) Å for [K(benzo-15-crown-5)$_2$][**1-C**]. Using the 3σ criterion, two of the three Mo−N bond lengths of **1-CH** are equivalent to those found in [K(benzo-15-crown-5)$_2$][**1-C**]. Since there is very little crystallographic difference between the two structures, it is difficult to draw conclusions about the Mo−C bond order based on crystallographic data alone. Such a situation has been encountered previously in a related system in which a *shorter* Mo−P bond length was observed for the phosphorus monoxide complex **1-PO** than for the terminal phosphide **1-P**.[15]

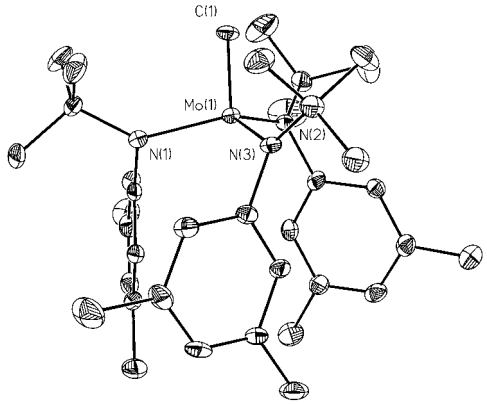

Figure 1. Thermal ellipsoid representation of **1-CH**. Ellipsoids are at the 35% probability level. Selected bond distances (Å) and angles (deg) Mo−C1 1.702(5), Mo−N1 1.981(4), Mo−N2 1.991(4), Mo−N3 1.964-(4), C1−Mo−N1 102.4(2), C1−Mo−N2 101.7(2), C1−Mo−N3 101.6-(2).

3. Solution ^{13}C NMR Spectra. A detailed ^{13}C NMR spectroscopic study of the ^{13}C-labeled carbide [**1**-^{13}**C**]$^-$ and its precursors pivalatocarbyne **1**-^{13}**COC(O)^{t}Bu** and methylidyne **1**-^{13}**CH** was undertaken to accrue insight into the properties of the molybdenum-bound carbon atom and accordingly into the nature of the Mo−C bonding. This study was facilitated by the ease of incorporating a ^{13}C label into the compounds through the use of 99% ^{13}CO in the preparation of carbonyl complex **1**-^{13}**CO**.[3] Noteworthy is the very large downfield shift of 501 ppm for [K(Kryptofix 222)][**1**-^{13}**C**]. The ^{13}C NMR shift for the

(11) Miller, R. L.; Wolczanski, P. T.; Rheingold, A. L. *J. Am. Chem. Soc.* **1993**, *115*, 10422.

(12) LaPointe, R. E.; Wolczanski, P. T.; Mitchell, J. F. *J. Am. Chem. Soc.* **1986**, *108*, 6382.

(13) Fickes, M. G.; Odom, A. L.; Cummins, C. C. *Chem. Commun.* **1997**, 1993−1994.

(14) Peters, J. C. Ph.D. Thesis, Massachusettes Institute of Technology, 1998.

(15) Johnson, M. J. A.; Odom, A. L.; Cummins, C. C. *J. Chem. Soc., Chem. Commun.* **1997**, 1523.

carbido carbon atom of [K(Kryptofix 222)][**1-C**] was reported originally as δ 488 ppm, this value being in error due to chemical exchange with small amounts of methylidyne **1-**^{13}**CH** present in the sample.[3] Details of said exchange process are discussed below.

Known compounds with large downfield ^{13}C NMR chemical shifts include the bridging cationic alkylidynes reported by Casey.[16,17] Terminal phosphido and nitrido molybdenum tris-anilido compounds, isolobal with [**1-C**]$^-$, display large downfield ^{31}P and ^{15}N NMR chemical shifts, respectively.[18,19] Pronouncedly larger in its downfield ^{13}C NMR shift is the ^{13}C signal for [K(Kryptofix 222)][**1-C**] in comparison with those for other molecules incorporating a one-coordinate carbon atom, including such examples as CO (δ 181),[20] [CN]$^-$ (δ 168), and CNMe (δ 158).[21] Not merely ascribable to the presence of negative charge is the dramatic downfield shift for the carbido carbon in [**1-**^{13}**C**]$^-$, since the chemical shift *difference* between it and that for the corresponding methylidyne **1-**^{13}**CH** (δ 288) of 213 ppm is substantially larger than the corresponding 49 ppm chemical shift difference between the signal for $Me(CH_2)_5$-CCH (δ 70.7) and the corresponding lithiated derivative (Me-$[CH_2]_5C\mathit{C}Li)_n$ (δ 118.8).[22] As will be seen below, the occurrence of a large downfield chemical shift is related to a large chemical shift anisotropy (CSA) distinguishing the parallel and the perpendicular shielding tensors along the molybdenum−carbon bond axis.

It is found that the carbido carbon ^{13}C NMR chemical shift is not greatly sensitive to the nature of the counterion. For example, in benzene solvent (**1-**^{13}**CK**)$_2$ and (**1-**^{13}**CLi**)$_n$ have ^{13}C NMR shifts of δ 482 and 470.1, respectively. Upon dissolving (**1-**^{13}**CK**)$_2$ in THF, two peaks are observed for the ^{13}C-labeled carbon, one at 489 ppm and the other at 501 ppm. Presumably, THF solvates some of the potassium ions leading to a mixture in solution of dimeric (**1-**^{13}**CK**)$_2$ and a monomeric, THF-solvated species, e.g. **1-**^{13}**CK**(**THF**)$_x$. Assuming that the peak at 489 ppm is the dimer and that the peak at 501 ppm is the monomeric THF solvated carbide species, it is possible to determine from ^{13}C NMR integration an equilibrium constant for the equation

$$2\ \textbf{1-}^{13}\textbf{CK}(\textbf{THF})_x \rightleftharpoons (\textbf{1-}^{13}\textbf{CK})_2$$

The integrations in the ^{13}C NMR spectrum are reliable measures of concentration because there is no nuclear Overhauser effect (nOe), due to the absence of protons directly bound to the ^{13}C nucleus in question, and because the acquisition time employed (0.8 s) is greater than 5 T_1 for both species.[23] At 0 °C, K_{eq} is found to be 22.5 M^{-1}, and upon cooling the solution, the equilibrium is found to favor the solvent-free form. From the temperature dependence of K_{eq} was determined $\Delta H = 13.3$ kJ mol^{-1} and $\Delta S = -23$ J mol^{-1} K^{-1}.

The observed $^1J_{CH}$ of 157 Hz for methylidyne **1-**^{13}**CH** is much smaller than is typical for sp-hybridized carbon centers. Generally, $^1J_{CH}$ is seen to increase with increasing s character in the C−H bond. A typical $^1J_{CH}$ value for an sp-hybridized carbon center is ca. 250 Hz. For example, $^1J_{CH}$ values are 251 and 269 Hz for phenylacetylene and hydrogen cyanide, respectively.[24] However, it has been noted previously that $^1J_{CH}$ coupling constants in transition metal methylidyne species are small, implying a limited amount of s character in the C−H bond.[25] More recently, Hopkins has reported vibrational spectroscopy of methylidyne complexes in work suggesting also that there is a limited amount of s character in the C−H bond.[26] The $^1J_{CH}$ value reported here for **1-**^{13}**CH** is larger than that of 138 Hz reported for the related tungsten methylidyne, HC≡W((Me$_3$-SiNCH$_2$CH$_2$)$_3$N).[27]

To investigate further the NMR parameters of the Mo−C multiply bonded compounds, and to optimize conditions for spectral data collection, the relaxation rates for the ^{13}C-labeled carbon nuclei were measured. All of the measured T_1 values are very short, which is particularly noteworthy for pivalatocarbyne **1-**^{13}**COC(O)**^{t}**Bu** and the carbide [K(Kryptofix 222)][**1-**^{13}**C**], compounds lacking protons on the ^{13}C nuclei, and hence having no ^{1}H−^{13}C dipole−dipole relaxation mechanism.[23] Observed T_1 values are 0.97, 0.63, and 0.14 s for **1-**^{13}**COC(O)**^{t}**Bu**, **1-**^{13}**CH**, and [K(Kryptofix 222)][**1-**^{13}**C**] at room temperature (ca. 25 °C) and 500 MHz. Other compounds lacking dipole−dipole relaxation often have very long ^{13}C T_1 values, an example being phenylacetylene, $HC_\alpha{\equiv}C_\beta Ph$, wherein the α and β carbons have T_1 values of 9.3 and 132.0 s, respectively.[28]

4. Solid-State ^{13}C NMR Spectra. As mentioned earlier, the terminal carbon atom in [**1-C**]$^-$ is associated with a ^{13}C NMR chemical shift of 501 ppm, such a shift being deshielded remarkably in relation to the typical ^{13}C NMR shift window for diamagnetic compounds. On the basis of previous observations involving terminal phosphido compounds including **1-P**,[18] the terminal ^{13}C nucleus in [**1-**^{13}**C**]$^-$ is expected to exhibit a large CSA. In addition, no $^1J_{MoC}$ was observed in the solution ^{13}C NMR spectra of the ^{13}C-labeled compounds considered here. This lack of $^1J_{Moc}$ data from solution ^{13}C NMR spectra is ascribable to the fact that $^{95/97}$Mo nuclei (^{95}Mo, $I = {}^5/_2$, 15.72%; ^{97}Mo, $I = {}^5/_2$, 9.46%) are often self-decoupled from the ^{13}C nuclei as a result of efficient $^{95/97}$Mo quadrupole relaxation in the liquid phase. In fact, in only one previous case has the *J*-coupling between ^{13}C and $^{95/97}$Mo nuclei been reported in the literature, the value in question being 68 Hz for the $^1J_{MoC}$ in Mo(CO)$_6$.[29,30] To investigate ^{13}C CSA and $^1J_{MoC}$ parameters for the compounds of the present work, solid-state ^{13}C NMR spectra were collected.

Displayed in Figure 2 are the ^{13}C CP/MAS NMR spectra of carbide [**1-**^{13}**C**]$^-$, pivalatocarbyne **1-**^{13}**COC(O)**^{t}**Bu**, and methylidyne **1-**^{13}**CH.** For all three compounds, the isotropic ^{13}C chemical shifts observed in the solid state are in excellent agreement with data obtained from solution spectra. In each of the three solid-state ^{13}C NMR spectra of Figure 2, the isotropic peak is flanked by a large number of spinning sidebands,

(16) Casey, C. P.; Meszaros, M. W.; Fagan, P. J.; Bly, R. K.; Marder, S. R.; Austin, E. A. *J. Am. Chem. Soc.* **1986**, *108*, 4043.
(17) Casey, C. P.; Gohdes, M.: A.; Meszaros, M. W. *Organometallics* **1986**, 5, 196.
(18) Wu, G.; Rovnyak, D.; Johnson, M. J. A.; Zanetti, N. C.; Musaev, D. G.; Morokuma, K.; Schrock, R. R.; Griffin, R. G.; Cummins, C. C. *J. Am. Chem. Soc.* **1996**, *118*, 10654.
(19) Laplaza, C. E.; Johnson, M. J. A.; Peters, J. C.; Odom, A. L.; Kim, E.; Cummins, C. C.; George, G. N.; Pickering, I. *J. J. Am. Chem. Soc.* **1996**, *118*, 8623.
(20) Ettinger, R.; Blume, P.; Patterson, A. *J. Chem. Phys.* **1960**, *33*, 1597.
(21) Maciel, G. E.; Beatty, D. A. *J. Phys. Chem.* **1965**, *69*, 3920.
(22) Seebach, D.; Hässig, R.; Gabriel, J. *Helv. Chim. Acta* **1983**, *66*, 308.
(23) Harris, R. K. *Nuclear Magnetic Resonance Spectroscopy*; Pitman Publishing Inc.: Boston1983.
(24) Maciel, G. E.; McIver, J. W.; Ostlund, N. S.; Pople, J. A. *J. Am. Chem. Soc.* **1970**, *92*, 1.
(25) Jamison, G. M.; Bruce, A. E.; White, P. S.; Templeton, J. L. *J. Am. Chem. Soc.* **1991**, *113*, 5057.
(26) Manna, J.; Dallinger, R. F.; Miskowski, V. M.; Hopkins, M. D. *J. Phys. Chem. B* **2000**, *104*, 10928.
(27) Schrock, R. R.; Seidel, S. W.; M6sch-Zanetti, N. C.; Dobbs, D. A.; Shih, K.; Davis, W. M. *Organometallics* **1997**, *16*, 5195.
(28) Levy, G. C. *J. Chem. Soc., Chem. Commun.* **1972**, 47.
(29) Mann, B. E. *J. Chem. Soc., Dalton Trans.* **1973**, 2012.
(30) Eichele, K.; Wasylishen, R. E.; Nelson, J. H. *J. Phys. Chem.* **1997**, *101*, 5463.

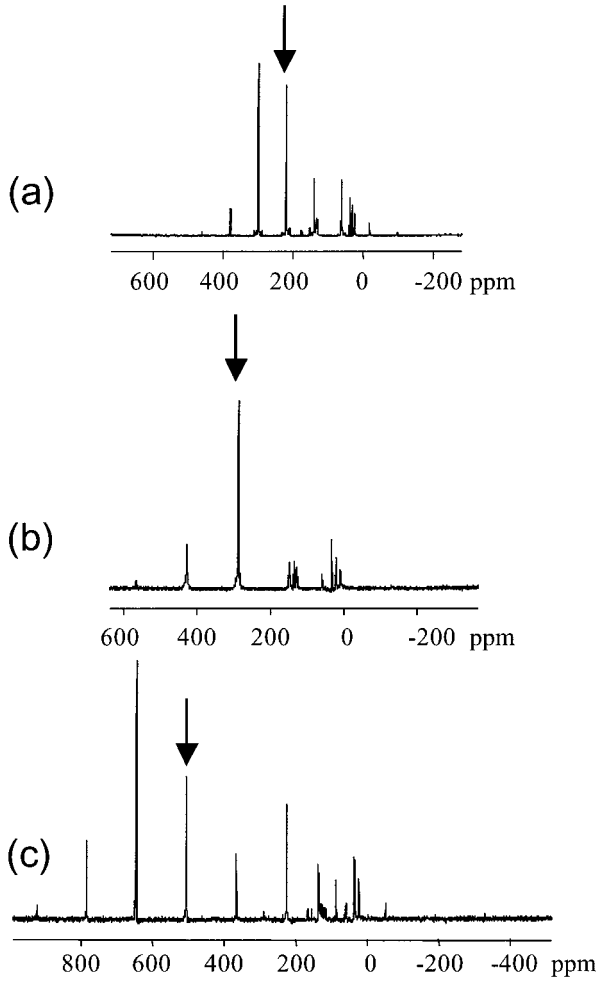

Figure 2. ^{13}C MAS NMR spectra of (a) **1**-^{13}**COC(O)^{t}Bu**, (b) **1**-^{13}**CH**, and (c) (**1**-^{13}**CK**)$_2$. The spectra were obtained at 4.7 T. The isotropic peaks are indicated.

indicating the presence of CSA, as discussed in more detail below. Close examination of the expanded isotropic regions of the ^{13}C NMR spectra (Figure 3) reveals interesting satellite peaks due to the *J*-coupling to $^{95/97}$Mo nuclei. The observed spectral features in the ^{13}C NMR spectra are similar to those observed in the ^{31}P NMR spectra of complexes containing ^{31}P−$^{95/97}$Mo spin pairs.[31] The detailed theory of the spectral analysis has been outlined in several studies.[32−34] Simulated ^{13}C NMR spectra also are shown in Figure 3. The values of $^{1}J_{MoC}$ were found to be 208, 130, and 60 (all ±5) Hz for pivalatocarbyne **1**-^{13}**COC(O)^{t}Bu**, methylidyne **1**-^{13}**CH**, and carbide anion [**1**-^{13}**C**]$^{-}$, respectively.

Another piece of new information garnered automatically from the spectral simulation is the molybdenum nuclear quadrupole coupling constant (NQCC).[33,34] For compounds [**1**-^{13}**C**]$^{-}$, pivalatocarbyne **1**-^{13}**COC(O)^{t}Bu**, and methylidyne **1**-^{13}**CH**, the e^2qQ/h (^{95}Mo) is found to be approximately −2.9 MHz. The ^{13}C CP/MAS spectra obtained at a higher field strength, 11.75 T, confirmed the *J*-coupling constants and the NQCC value.

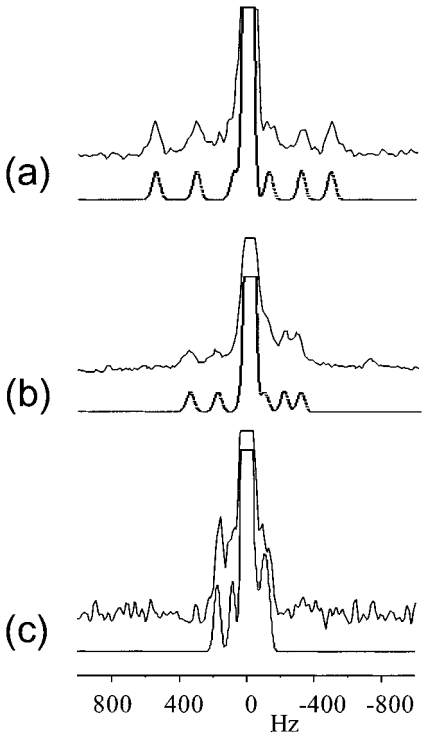

Figure 3. The isotropic regions of the observed (upper trace) and calculated (lower trace) ^{13}C MAS spectra of (a) **1**-^{13}**COC(O)^{t}Bu**, (b) **1**-^{13}**CH**, and (c) (**1**-^{13}**CK**)$_2$. The spectra were obtained at 4.7 T.

5. Parallelism between M−C and M−P Multiple Bonds. Since it is difficult to observe any *J*-coupling involving $^{95/97}$Mo nuclei from solution NMR studies, relevant data in the literature for comparison purposes are essentially nonexistent. However, it should be noted that several examples of phosphido complexes, each described as containing a tungsten−phosphorus triple bond, have been reported recently along with their corresponding $^{1}J_{WP}$ values.[35−38] Therefore, the possible parallelism between metal−carbon and metal−phosphorus multiple bonds was considered. Such a parallelism is expected on the basis of the diagonal relationship between C and P.[39] To make the comparison meaningful, one uses the reduced spin−spin coupling *K*, defined by the following equation:[23]

$$^{1}K_{XM} = \frac{4\pi^2}{h\gamma_x\gamma_m}{}^{1}J_{XM}$$

with the unusual dimension of N Å^{-2} m^{-3}. Shown in Figure 4 is the plot of the X-nucleus chemical shift versus reduced spin−spin coupling constant, $^{1}K_{XM}$, for these two classes of complexes. In general, the values for $^{1}K_{MoC}$ are smaller than $^{1}K_{WP}$ values, which is consistent with the general trend found for spin−spin coupling constants between directly bonded nuclei.[40] The most interesting feature in Figure 4 is that the two sets of data are parallel to one another. In both cases, $^{1}K_{XM}$ increases with the chemical shielding at the X-nucleus, corresponding to

(31) Lindner, E.; Fawzi, R.; Mayer, H. A.; Eichele, K. W. H. *Organometallics* **1992**, *11*, 1033.
(32) Gobetta, R.; Harris, R. K.; Apperley, D. C. *J. Magn. Reson.* **1992**, *96*, 119.
(33) Eichele, K.; Wasylishen, R. E.; Corrigan, J. F.; Doherty, S.; Sun, Y.; Carty, A. J. *Inorg. Chem.* **1993**, *32*, 121.
(34) Wasylishen, R. E.; Wright, K. C.; Eichele, K.; Cameron, T. S. *Inorg. Chem.* **1994**, *33*, 407.
(35) Zanetti, N.; Schrock, R. R.; Davis, W. M. *Angew. Chem., Int. Ed. Engl.* **1995**, *34*, 2044.
(36) Scheer, M.; Schuster, K.; Budzichowski, T. A.; Chisholm, M. H.; Streib, W. E. *J. Chem. Soc., Chem. Commun.* **1995**, 1671.
(37) Scheer, M.; Mller, J.; Haser, M. *Angew. Chem., Int. Ed. Engl.* **1996**, *35*, 2492.
(38) Mösch-Zanetti, N. C.; Schrock, R. R.; Davis, W. M.; Wanninger, K.; Seidel, S. W.; O'Donoghue, M. B. *J. Am. Chem. Soc.* **1997**, *119*, 11037.
(39) Regitz, M.; Scherer, O. J.; Appel, R. *Multiple Bonds and Low Coordination in Phosphours Chemistry*; Stuttgart: New York,1990.
(40) Jameson, C. J.; Gutowsky, H. *S. J. Chem. Phys.* **1969**, *51*, 2790.

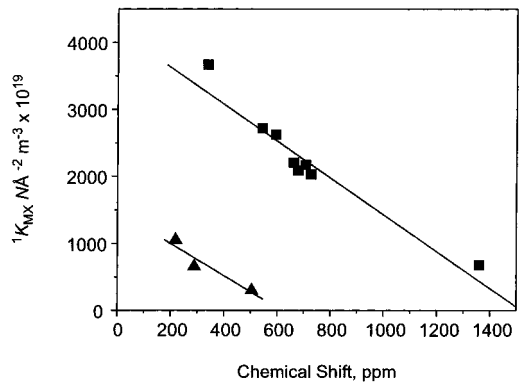

Figure 4. Plot illustrating the parallelism of NMR parameters between metal-*C* (triangles) and metal-*P* multiply bonded (squares) compounds.

a decrease in the chemical shift value. This observation suggests strongly that the nature of these two types of chemical bonds is similar.

A recent Pair of Electron Sharing Hybrid Orbital (PESHO) analysis has indicated that the P−W bond consists largely of one $d_\sigma-p_\sigma$ bond and two $d_\pi-p_\pi$ bonds.[37] Similarly, the decrease in $^1J_{MoC}$ on going from **1-**^{13}**COC(O)**^{t}**Bu** and **1-**^{13}**CH** to [**1-**^{13}**C**]$^-$ can be attributed to progressively diminished involvement of the carbon 2s electrons in the molybdenum−carbon multiple bond. Combined with the observation of an unusually small $^1J_{CH}$ in methylidyne **1-**^{13}**CH**, it can be concluded that in [**1-**^{13}**C**]$^-$ the carbon pair of 2s electrons is localized largely at the carbon atom.

6. ^{13}C CSA Parameters. In general, it is possible to obtain three principal components of a chemical shift tensor from an analysis of spinning sidebands. However, it is also well-known that, for a chemical shift tensor close to axial symmetry, spinning sideband analysis often yields inaccurate results.[41] For this reason, ^{13}C NMR spectra were obtained for stationary samples.

Depicted in Figure 5 are the ^{13}C NMR spectra for stationary powder samples of (**1-**^{13}**CK**)$_2$, **1-**^{13}**COC(O)**^{t}**Bu**, and **1-**^{13}**CH,** together with corresponding simulated spectra. The signal not represented in the simulated spectra is due to the natural abundance ^{13}C from the ligands. From these spectra, the principal components can be determined accurately as given in Table 1.

It is noted that the ^{13}C chemical shift tensors for the three compounds studied exhibit axial symmetry, consistent with the expectation from their crystal structures. The span of the ^{13}C chemical shift tensor in [**1-**^{13}**C**]$^-$, 806 ppm, is apparently the largest among diamagnetic compounds so far studied. It is clear also from Table 1 that the significant deshielding effect observed in (**1-**^{13}**CK**)$_2$ arises from the large paramagnetic shielding along directions perpendicular to the Mo≡C bond axis, i.e., δ_{11} and δ_{22}. In contrast, the shielding along the Mo≡C bond, δ_{33}, is similar for the three compounds studied here, indicating that the paramagnetic shielding contribution is negligible along the nearly cylindrical Mo≡C bond axis. Reminiscent of the circumstance for phosphido compounds such as **1-P**, the observation of a remarkably large paramagnetic shielding in (**1-**^{13}**CK**)$_2$ is suggestive of the presence of a low-lying Mo−C π^* orbital (LUMO) in conjunction with a high-lying HOMO of σ symmetry with respect to the MoC bond axis.

7. DFT Calculations. To investigate further the electronic structure of the Mo−C multiply bonded compounds here considered, DFT calculations on appropriate model systems were carried out using the Amsterdam Density Functional theory program suite.[42−44] Initial calculations focused on dimethylamido based model systems, e.g. [CMo(NMe$_2$)$_3$]$^-$, but it was found that the results and interpretations differed insignificantly from those based on simple amido-based model systems, e.g. [CMo(NH$_2$)$_3$]$^-$. The latter computationally less-intensive systems therefore are the only ones to be discussed in detail here.

Calculated core bond lengths and angles for both carbide [CMo(NH$_2$)$_3$]$^-$ and methylidyne HCMo(NH$_2$)$_3$ matched reasonably well the crystallographically determined values for [**1-C**]$^-$ and **1-CH**, respectively, as indicated by the values in Table 2.

Hirshfeld charges were used as an indication of the relative charge distribution in the model systems [CMo(NH$_2$)$_3$]$^-$ and HCMo(NH$_2$)$_3$. Accordingly the carbon atom in the latter methylidyne carries a charge of −0.2379 while the carbon atom in the former anionic carbide carries a calculated charge of −0.5334. Such an increase in negative charge upon deprotonation is, of course, expected for the carbon atom in question. In addition, the charge on the molybdenum center decreases

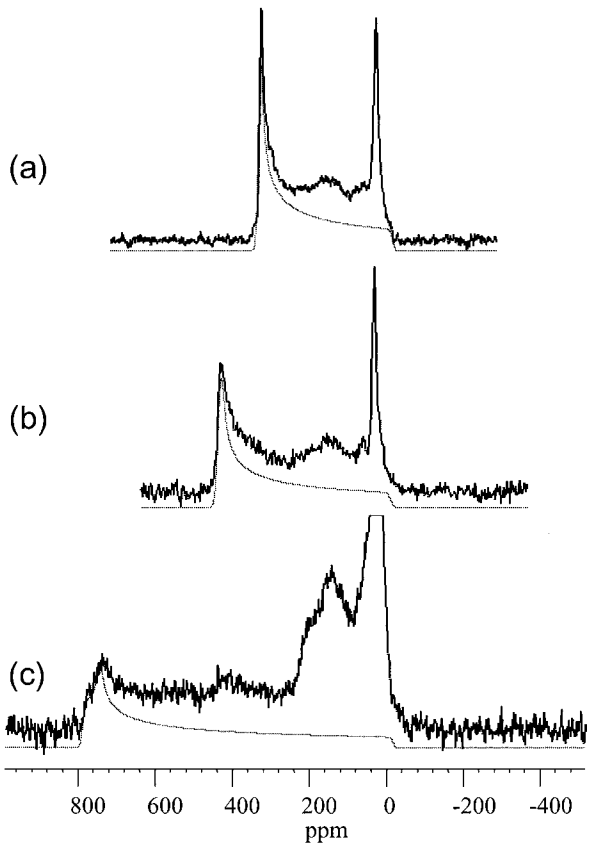

Figure 5. Observed (solid line) and calculated (dashed line) ^{13}C NMR spectra of stationary powder samples of (a) **1-**^{13}**COC(O)**^{t}**Bu**, (b) **1-**^{13}**CH**, and (c) (**1-**^{13}**CK**)$_2$.

Table 1. Solid-State ^{13}C NMR Data

	δ_{iso}[a]	δ_{11}[b]	δ_{22}	δ_{33}	κ[c]	Ω[d]	$^1J_{MoC}$[e]	$^1K_{MoC}$[f]
1-^{13}**COC(O)**^{t}**Bu**	218	334	334	−13	1.00	347	208	1053
1-^{13}**CH**	288	437	437	−10	1.00	447	130	658
(1-^{13}**CK)$_2$**	504	788	742	−18	0.88	806	60	304

[a] Chemical shifts are in ppm and are referenced to TMS. [b] Chemical shift tensor components are reported to ±2 ppm. [c] Skew = $3(\delta_{22} - \delta_{iso})/(\delta_{11} - \delta_{33})$. [d] Span = $\delta_{11} - \delta_{33}$. [e] *J* couplings are reported to ±5 Hz. [f] The reduced indirect spin−spin coupling constant *K* has units of N Å^{-2} m^{-3} × 10^{19}.

(41) Herzfeld, J.; Berger, A. E. *J. Chem. Phys.* **1980**, *73*, 6021.
(42) Baerends, E. J.; et al. *Chem. Phys.* **1973**, *2*, 41.
(43) te Velde, G.; Baerands, E. J. *J. Comput. Phys.* **1992**, *99*, 84.
(44) Guerra, C. F.; et al. *METECC-95* **1995**, 305.

Table 2. Comparison of DFT[a] and Experimental[b] Structures[c]

	$[CMo(NH_2)_3]^-$	$[\mathbf{1\text{-}C}]^-$	$HCMo(NH_2)_3$	**1-CH**
d_{Mo-C}	1.74	1.71	1.74	1.80
d_{Mo-N}	2.02	2.01	1.98	1.98
$\angle_{C-Mo-N}$	101.3	103.5	102.0	101.9

[a] Geometry optimizations employed a C_3 symmetry constraint. [b] Crystallographic C_3 symmetry was not present for either of the experimentally determined structures. Average values therefore are given for relevant metrical parameters. [c] Distances are provided in Å, while angles are given in deg.

from 0.5992 in the methylidyne complex to 0.3628 for the anionic carbide. While the latter trend is a necessary consequence of charge conservation, it may be taken as an indication that the Mo center contributes to stabilization of the anion by acquiring a significant fraction of the total negative charge.

In view of the solid-state NMR results discussed above, the orbital structure of $[CMo(NH_2)_3]^-$ was investigated with the goal of acquiring information concerning the Mo−C bond order. Mulliken Mo−C overlap populations (OPs)[45] were calculated for a series of complexes anticipated to exhibit a smooth gradation in Mo−C bond order: the complexes being triplet $H_3CMo(NH_2)_3$, doublet $H_2CMo(NH_2)_3$, singlet $HCMo(NH_2)_3$, and singlet $[CMo(NH_2)_3]^-$. A gradual increase in Mo−C overlap population indeed was observed across the series, the values obtained being 0.1545, 0.2808, 0.4462, and 0.5795, going from methyl, through methylidene and methylidyne, and finally to the anionic carbide.

The feature of greatest interest here is the interpretation of the *increase* in metal−carbon OP on going from methylidyne to the anionic carbide. An obvious interpretation is that an increase in Mo−C bonding accompanies deprotonation of the neutral methylidyne complex. Such an increase can be taken to reflect delocalization (via added bonding) of the added negative charge. As an aid to interpretation, carbon−carbon OPs were calculated for the following series of organic compounds: C_2H_6, C_2H_4, C_2H_2, and $[C_2H]^-$, the obtained values being 0.3504, 0.5900, 0.8296, and 1.2210.

As there is a congruence in the OP trends for both the organic and the organometallic bond types, it can be concluded that the increase in OP upon deprotonation to form the terminal carbide substituent is in both cases due to the accompanying acquisition of negative charge. In effect, the calculations reflect the fact that the formal $[C]^{4-}$ ligand is a stronger donor than is the formal $[CH]^{3-}$ ligand, regardless of whether said ligand is bonded to an organic or to a transition-metal fragment. In both cases, therefore, the multiple bond can be taken to have a greater bond order for the anionic terminal carbide than for the neutral methylidyne. Other results might be anticipated if one were to compare a neutral methylidyne complex with an isoelectronic *neutral* terminal carbide species, but such a comparison is outside the scope of the present study.

8. Brønsted Acidity of Methylidyne 1-CH. In the reported sequence for the synthesis of methylidyne **1-CH** (Scheme 1),[3] a mixture containing sodium salts of the carbide anion $[\mathbf{1\text{-}C}]^-$ is quenched by addition of an excess of acetonitrile, indicating that the anionic carbide is sufficiently basic to deprotonate CH_3CN. Furthermore, the preparation of potassium salts of $[\mathbf{1\text{-}C}]^-$ involved the deprotonation of methylidyne **1-CH** by the strong base benzylpotassium. It can be inferred therefore that the pK_a for methylidyne **1-CH** is approximately between 31 and 41, using the pK_a values for acetonitrile and toluene taken from the acidity scale developed by Bordwell for DMSO solvent.[47]

It has been seen, however, that observed pK_a values may be sensitive to factors including choice of solvent and nature of counterion. For example, the pK_a of phenylacetylene was found to be 28.7 in DMSO as compared with 31.1 in THF, the latter value being obtained with an encrypted lithium counterion.

A series of measurements were made in which the potassium salt $(\mathbf{1\text{-}CK})_2$ was dissolved in THF and an organic acid of known pK_a was added. After equilibration and removal of THF from the mixtures thereby obtained, ^{1}H NMR spectra were collected in C_6D_6 solvent. It was found that phenylacetylene converted the anionic carbide $[\mathbf{1\text{-}C}]^-$ quantitatively to its conjugate acid, methylidyne **1-CH**. Morris has recently reported a new THF acidity scale utilizing ^{1}H and ^{31}P NMR spectroscopy. However, the rapid rate of proton-transfer self-exchange in THF, described in the following section, prevented the use of this solvent for pK_a measurements.

It was found also that the potassium salt of triphenylmethide ion was sufficiently basic to effect partial conversion of **1-CH** to carbide anion $[\mathbf{1\text{-}C}]^-$, when employed stoichiometrically. Similar spectra were obtained for the reverse reaction, namely the addition of the potassium carbide to a stoichiometric amount of triphenylmethane, with both carbon acids and their conjugate bases being observed in near equal amounts. These results suggest that the acidity of Ph_3CH (pK_a = 30.6 in DMSO[47] and 30.8 in THF[48]) is very similar to that of methylidyne **1-CH**. Problematic in this study was the propensity of carbide $[\mathbf{1\text{-}C}]^-$ to become protonated, producing methylidyne **1-CH** over time in solution at 25 °C. For example, although benzylpotassium is a sufficiently strong base to deprotonate **1-CH** in THF, a toluene/THF mixture was found slowly to protonate $[\mathbf{1\text{-}C}]^-$ (potassium salt), possibly due to the presence of trace protic impurities or else by an unknown mechanism. On the other hand, a THF solution of the potassium carbide exhibited no decomposition when stored at 25 °C for 16 h.

9. Proton-Transfer Self-Exchange Kinetics. There is an extensive body of literature pertaining to the rates of proton-exchange reactions involving carbanions, and to the factors governing these rates. While proton-exchange reactions involving hydroxylic or amino functionalities typically are associated with diffusion-controlled rates, corresponding exchange rates for weakly acidic C−H groups are known to span 10 orders of magnitude.[50]

Proton transfer becomes slow when an anionic proton acceptor is capable of charge delocalization.[5] The latter theory has been developed extensively by Bernasconi as the principle of nonperfect synchronization.[51−52] The theory states that a product-stabilizing factor that develops after the transition state lowers k_0, the intrinsic rate constant, in the absence of a thermodynamic driving force. Examples of product stabilizing factors that may develop late along a reaction coordinate include resonance, charge delocalization, and solvation.

To determine the intrinsic rate of a proton-transfer reaction, kinetic and thermodynamic factors must be separated. One approach is to measure the rate of transfer involving a variety of bases, thereby gaining information from which the intrinsic rate may be extracted. A more desirable method is directly to measure the rate of a self-exchange reaction. Proton NMR

(45) Mulliken, R. S. *J. Chem. Phys.* **1955**, *23*, 1833.
(46) Chen, Y.; Petz, W.; Frenking, G. *Organometallics* **2000**, *19*, 2698.
(47) Bordwell, F. G. *Acc. Chem. Res.* **1988**, *21*, 456.
(48) Antipin, I. S.; Gareyev, R. F.; Vedernikov, A. N.; Konovalov, A. I. *J. Phys. Org. Chem.* **1994**, *7*, 181.
(49) Abdur-Rashid, K.; Fong, T. P.; Greaves, B.; Gusev, D. G.; Himman, J. G.; Landau, S. E.; Lough, A. J.; Morris, R. H. *J. Am. Chem. Soc.* **2000**, *122*, 9155.
(50) Bernasconi, C. F. *Adv. Phys. Org. Chem.* **1992**, *27*, 119.
(51) Bernasconi, C. F. *Acc. Chem. Res.* **1987**, *20*, 301.
(52) Bernasconi, C. F. *Acc. Chem. Res.* **1992**, *25*, 9.

spectroscopy often constitutes a convenient method for the interrogation of degenerate proton-transfer reactions, but ^{13}C NMR spectroscopy has been employed also, for example, in a study concerning the rates of HCN/cyanide proton-exchange reactions in aqueous media.[53]

Carbon-13 NMR spectroscopy proved to be suitable for the study of proton-exchange rates involving methylidyne **1**-^{13}**CH** and carbide anion [**1**-^{13}**C**]$^-$. NMR data obtained for anion [**1**-^{13}**C**]$^-$, as its potassium Kryptofix 222 salt, are indicative of rapid proton-transfer reactivity in the presence of trace amounts of methylidyne **1**-^{13}**CH**. This is why the originally reported ^{13}C chemical shift for the same salt in THF was 482.8 ppm, the peak width $\Delta\nu_{1/2}$ having been given as 1400 Hz.[3] Acquisition of [K(Kryptofix 222)][**1**-^{13}**C**] spectra in the presence of small amounts of benzyl potassium allowed for the limiting chemical shift for the carbido carbon of [K(Kryptofix 222)][**1**-^{13}**C**] to be determined as 501 ppm, the peak width in this case being relatively narrow ($\Delta\nu_{1/2}$ = 46 Hz). Benzylpotassium in the previous experiment serves to scavenge traces of methylidyne **1**-^{13}**CH**. It is fortuitous that the chemical shifts for the ^{13}C-labeled positions in carbide [K(Kryptofix 222)][**1**- ^{13}**C**] and methylidyne **1**-^{13}**CH** are so disparate, because this circumstance allows for very fast rates of proton exchange to be measured by line-shape analysis. On the basis of the 213 ppm separation in chemical shifts, and a spectrometer operating at 125 MHz for ^{13}C NMR, coalescence of the two signals is expected when the exchange lifetime, τ, is ca. 6×10^{-6} s.

For a two-component system undergoing degenerate chemical exchange the observed NMR spectrum depends on the lifetime τ, the relative concentration of the two species, T_2 relaxation times, and the limiting chemical shift values.[54] In the present study, chemical shift and T_2 relaxation parameters were measured independently in the absence of exchange.[54] Simulated spectra were produced using appropriate line-shape equations.[54] Relative concentrations of the two species as determined from experimental spectra were used as a starting point for the simulations, but the extreme sensitivity of carbide [**1**-^{13}**C**]$^-$ to protonation by trace impurities necessitated the inclusion of this quantity as a variable parameter. Peak widths obtained from simulated spectra were compared to those observed experimentally, this procedure constituting the means for determination of the lifetime, τ.

At room temperature, ^{13}C NMR spectra for mixtures of [K(Kryptofix 222)][**1**-^{13}**C**] and **1**-^{13}**CH** in THF exhibit coalescence behavior, such that only a very broad signal is observed. At lower temperatures, however, the rate of proton exchange diminishes and accordingly it becomes possible to distinguish individual peaks for both species. Figure 6 is illustrative of the system's temperature-dependent behavior. For a sample containing similar amounts of [K(Kryptofix 222)][**1**-^{13}**C**] and **1**-^{13}**CH** it was possible to detect both peaks at low temperature. No peaks were observed at room temperature, which is consistent with the nearly flat simulated spectrum. To circumvent this problem and to measure a room-temperature rate constant, it was necessary to prepare samples with either high methylidyne or high carbide concentrations.

The rate constant was determined by assuming that the reaction is first order in each reactant. The rate constant was obtained from the expression $k = 1/(\tau[C])$, where [C] is the total concentration of both molybdenum-containing species. This assumption was validated by preparing samples at several different total molybdenum concentrations, and relative concentrations of **1**-^{13}**CH** and [K(Kryptofix 222)][**1**-^{13}**C**]. The data are shown in Table 3. The rate constant obtained at 20 °C is 7×10^6 M^{-1} s^{-1}. At −60 °C the rate constant shrinks to 4×10^5 M^{-1} s^{-1}, and at −90 °C it is 1×10^5 M^{-1} s^{-1}. The activation parameters obtained from the Arrhenius plot suggest E_a = 17 kJ/mol.

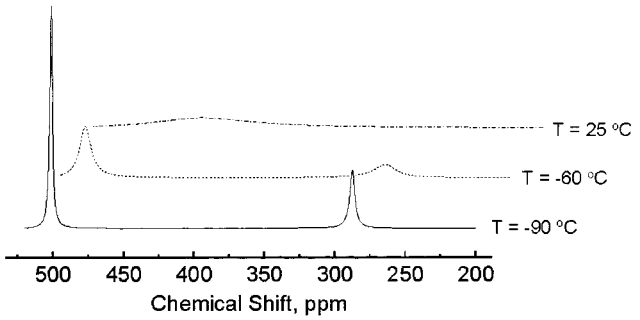

Figure 6. Temperature dependence of the proton-transfer self-exchange kinetics. The spectra are calculated for a total molybdenum concentration of 27 mM, and a [K(Kryptofix 222)][**1**-^{13}**C**]/**1**-^{13}**CH** ratio of 1.5. At −90 °C the lifetime was calculated at $\tau = 4 \times 10^{-4}$ s and at −60 °C the lifetime was calculated at $\tau = 9 \times 10^{-5}$ s. Experimental spectra corresponding to −90 and −60 °C were collected and fit to these parameters (Supporting Information). At room temperature $\tau = 5 \times 10^{-6}$ s (dash-dot line). No spectrum was observed at room temperature.

Table 3. Room Temperature Kinetic Data[a]

total [Mo]	[**1-CH**]/*M*[**1-C**][b]	τ_c	k[d]
30	5.7	5	7
25	4	6	7
15	20	10	7

[a] Concentrations in mM. [b] M = [K(Kryptofix 222)]. [c] Lifetime, τ in s $\times 10^{-6}$. [d] Second-order rate constant k, in M^{-1} s^{-1} $\times 10^6$.

The rate of self-exchange between [K(Kryptofix 222)][**1-C**] and **1-CH** is very fast for proton exchange in a carbon acid/base pair,[5] suggesting that there is not an extensive amount of charge delocalization onto the ligands.

Solvent effects due to the use of THF could cause significant differences relative to the aqueous solutions normally used for proton-transfer studies. The principle of nonperfect synchronization also is valid in the gas phase,[55,56] suggesting that even without a strong solvent effect we would expect a slower rate if a significant amount of charge were being delocalized onto the ligands. The implication that the developing negative charge density remains localized in the Mo−C bond upon deprotonation is consistent with the solid-state NMR data and the DFT calculations. The rates measured in this study are slower than those found for the analogous chemistry involving phenylacetylene, which by tritium tracer studies has been estimated to occur at the diffusion limit.[57] Significantly, the rates measured in this study for the exchange of [K(Kryptofix 222)][**1-C**] and **1-CH** are very close to those measured for hydrogen cyanide. A ^{13}C NMR exchange study has found the self-exchange rate constant for HCN/CN$^-$ to be 3.1×10^6 M^{-1} s^{-1} in an aqueous solution 1 M in $NaClO_4$.[53] This value for the hydrogen cyanide self-exchange rate constant is slightly higher than that obtained by Bedner and Jencks.[58−60]

(53) Banyai, I.; Blixt, J.; Glaser, J.; Toth, I. *Acta Chim. Scand.* **1992**, *46*, 142.
(54) Sandstrom, J. *Dynamic NMR Spectroscopy;* Academic Press: New York, 1982.
(55) Bernasconi, C. F.; Wenzel, P. J. *J. Am. Chem. Soc.* **1996**, *118*, 10494.
(56) Bernasconi, C. F.; Wenzel, P. J. *J. Am. Chem. Soc.* **1994**, *116*, 5405.
(57) Halevi, E. A.; Long, F. A. *J. Am. Chem. Soc.* **1961**, *83*, 2809.
(58) Bednar, R. A.; Jencks, W: P. *J. Am. Chem. Soc.* **1985**, *107*, 7117.
(59) Bedner, R. A.; Jencks, W. P. *J. Am. Chem. Soc.* **1985**, *107*, 7126.
(60) Bedner, R. A.; Jencks, W. P. *J. Am. Chem. Soc.* **1985**, *107*, 7135.

Scheme 2

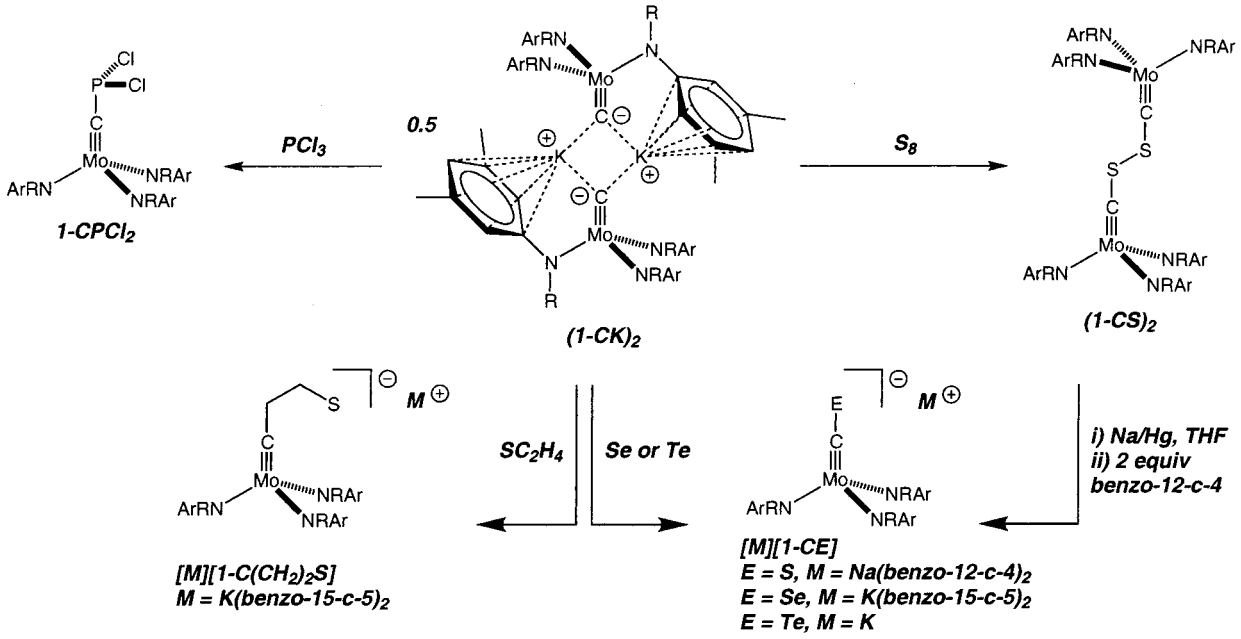

10. Nucleophilic Character of [1-C]$^-$. A survey of the nucleophilic reactivity of [**1-C**]$^-$ is summarized in Scheme 2. Having deoxygenated carbonyl **1-CO** en route to the isolation of [**1-C**]$^-$, it was deemed of interest to prepare heteroatom-substituted molybdenum alkylidynes involving the heavier chalcogenides. Elemental S, Se, and Te were found to react with (**1-CK**)$_2$ in diethyl ether, ultimately affording anionic thiocarbonyl,[61] selenocarbonyl,[62,63] and tellurocarbonyl complexes, respectively.[62] Isolation of the yellow seleno- and tellurocarbonyls (**1-CEK**)$_n$ (E = Se, Te; *n* is likely to be 2), proved to be straightforward. Although methylidyne **1-CH** is generated as an impurity upon addition of excess Se and Te to cold ethereal solutions of (**1-CK**)$_2$, the hydrocarbon insolubility of (**1-CEK**)$_n$ rendered them easily purified by washing with pentane. A ^{13}C NMR signal at 271.9 ppm was assigned to (**1-CSeK**)$_n$, while the corresponding signal for (**1-*C*TeK**)$_n$ was located at 252.6 ppm. The ion-separated salt [K(benzo-15-crown-5)$_2$][**1-CSe**] was prepared by addition of 2 equiv of benzo-15-crown-5 to a solution of (**1-CSeK**)$_n$, and its structure was confirmed in preliminary fashion by a single-crystal X-ray diffraction study.[14]

The isolation of [**1-CS**]$^-$ salts in pure form was a more interesting problem. Elemental sulfur reacted readily with (**1-CK**)$_2$ to form the orange, highly pentane-soluble bridged disulfide complex (**1-CS**)$_2$, the species exhibiting a ^{13}C NMR Mo*C*-S signal at 253.8 ppm. The yellow ion pair (**1-CSNa**)$_n$ was obtained subsequently from in situ generation of (**1-CS**)$_2$ followed by reduction with Na/Hg. Sodium thiocarbonyl (**1-CSNa**)$_n$ is identified with a ^{13}C NMR signal at 292.4 ppm and could be converted to the ion-separated salt [Na(12-crown-4)$_2$]-[**1-CS**] by addition of 2 equiv of 12-crown-4.

Two potential modes of reactivity of ethylene sulfide with carbidomolybdenum anion [**1-C**]$^-$ were foreseen, these being transfer of the sulfur atom to the carbido carbon to form the thiocarbonyl or nucleophilic attack by the carbide to form a ring-opened product. The latter proved to obtain, as the observed product stemmed from ring-opening of ethylene sulfide to give (**1-CCH$_2$CH$_2$SK**)$_n$, a species potentially useful as a metalloligand in transition metal thiolate chemistry. A further example of nucleophilic behavior on the part of [**1-C**]$^-$ was observed in the reaction of (**1-CK**)$_2$ with PCl_3. Clean monosubstitution was found to dominate, giving **1-PCl$_2$** in 53% isolated yield. Compound **1-CPCl$_2$** exhibits a ^{13}C NMR shift for MoCP at 294.6 ppm with $^1J_{CP}$ being 144 Hz. Dichlorophosphinocarbyne **1-CPCl$_2$** represents an intriguing platform for the construction of low-coordinate phosphorus compounds supported by the sterically demanding CMo(N[R]Ar)$_3$ substituent.

3. Concluding Remarks

Herein has been presented extensive characterization of a novel carbidomolybdenum anion. While other one-coordinate carbon bases (cyanide, acetylide) exhibit similar pK_a and proton-transfer rate profiles, the electronic structure of the anion of interest here clearly is more complex. The latter complexity has been unraveled in part herein via a study employing data from solid-state NMR investigations and solution NMR line shape data probing proton-transfer kinetics, in addition to structural information from X-ray crystallography and density functional theory calculations. A key conclusion is that the bonding paradigm advanced earlier for analogous phosphidometal systems extends nicely to their carbidometal relatives.[18] On the basis of such analogies, one expects to find the set of known *terminal* carbidometal functionalities growing as the field of metal−carbon multiple bonds continues to develop.[64−67] Finally underscored should be the potential synthetic *utility* of the terminal carbidometal functionality, since the same may be employed to give elaborate carbynes unavailable by other methods.

6. Experimental Procedure

1. General Considerations. All synthetic work and sample preparation was done in a Vacuum Atmospheres glovebox using standard techniques for the manipulation of air-sensitive compounds. Solvents

(61) Broadhurst, P. V. *Polyhedron* **1985**, *4*, 1801.
(62) Clark, G. R.; Marsden, K.; Rickard, C. E. F.; Roper, W. R.; Wright, L. J. *J. Organomet. Chem.* **1988**, *338*, 393.
(63) Clark, G. R.; James, S. M. *J. Organomet. Chem.* **1977**, *134*, 229.
(64) Schrock, R. R. *Acc. Chem. Res.* **1986**, *19*, 342.
(65) Schrock, R. *Acc. Chem. Res.* **1990**, *23*, 158.
(66) Feldman, J.; Schrock, R. *Prog. Inorg. Chem.* **1991**, *39*, 1.
(67) Trnka, T.; Grubbs, R. *Acc. Chem. Res.* **2001**, *34*, 18.

were dried according to standard procedures.[68] $Mo(N[R]Ar)_3$ (**1**) was prepared according to the literature procedure.[19] Diisopropylamine and phenylacetylene were dried by storing over 3 Å sieves, while triphenylmethane and Kryptofix 222 were dried by dissolving in THF and passing the solution through a small column of alumina. ^{13}CO was purchased from Cambridge Isotope Laboratories, Inc.; all other materials were obtained from standard sources. NMR data were collected on Varian VXR-500 or Varian Unity-300 spectrometers and IR data were collected on a Biorad 135 Series FTIR spectrometer. Magnetic susceptibilities were determined by the method of Evans.[69,70] Microanalyses were obtained by Microlytics, South Deerfield, MA. All NMR samples for relaxation parameters and kinetic studies were contained in flame-sealed tubes and interrogated using a Varian VXR-500 spectrometer. All samples were referenced to residual solvent protons, and spectra of samples in protio solvents were obtained without a lock.

2. Solid-State NMR. Solid-state NMR spectra were obtained on Bruker Avance-500 and ASX-200 NMR spectrometers operating at 500 and 200 MHz for protons, respectively. All ^{13}C chemical shifts were referenced to TMS using adamantane as a secondary external reference sample. Powder samples were packed into zirconium oxide rotors (4 mm o.d.) in a drybox. Typical sample spinning frequencies for experiments are 4−10 kHz. The recycle time was 10 s. Spectral analysis was carried out with the WSOLIDS program package kindly provided by Dr. Klaus Eichele and Professor Rod Wasylishen (Dalhousie University).

3. DFT Calculations. Calculations were performed on an SGI Indy workstation using the Amsterdam Density Functional Package employing Becke and Perdew gradient corrections (GGA) and the VWN local density approximation (LDA).[71−73] A scalar relativistic correction was also included for the Mo, C, and N atoms. Molybdenum was treated using a triple-ζ quality basis set including polarizations with up to the 3d orbitals frozen. Carbon was also treated at the triple-ζ level including polarizations with its ls electrons frozen. Nitrogen was treated using a double-ζ basis (with polarizations) and the ls frozen core. Hydrogen was treated at the triple-ζ level (with spin polarizations). All geometries were optimized in C_{3V} symmetry.

4. X-ray Structure of 1-^{13}CH. Colorless crystals were grown from a concentrated diethyl ether solution at −35 °C. The crystals were moved quickly from a vial and attached to a glass fiber. X-ray data were collected on a Siemens Platform goniometer with a charge coupled device (CCD) detector. The structure was solved by direct methods (Shelxtl version 5.0, G. M. Sheldrick and Siemens Industrial Automation Inc., 1995). Crystal and refinement data: $M_w = 637.78$ for $C_{37}H_{55}MoN_3$, monoclinic, $P2_1/n$, $a = 11.256(2)$ Å, $b = 17.278(7)$ Å, $c = 18.626(7)$ Å, $\alpha = 90°$, $\beta = 100.18(2)°$, $\gamma = 90°$, $V = 3565(2)$ Å^3, $Z = 4$, $D_{calc} = 1.188$ g·cm^{-3}, absorption coefficient = 0.395 mm^{-1}, $F(000) = 1360$, number of reflections collected = 14191, number of independent reflections = 5142, GOF = 1.115, $R = 0.0552$, $wR_2 = 0.1240$.

5. Synthesis of 1-^{13}CO. A 250 mL round-bottomed Schlenk flask was charged with a stir bar and **1** (2.736 g, 4.256 mmol). THF (60 mL) was added and the flask was evacuated and cooled to −78 °C and then exposed to 500 Torr of ^{13}CO gas (2 molar equiv in total). The reaction vessel was allowed to warm gradually to 22 °C during which time the solution turned a dark brown. The solvent was removed in vacuo. Hexamethyldisiloxane (15 mL) was added to the crude solid and the mixture was stirred vigorously. The undissolved material was collected on a sintered glass frit, washed with hexamethyldisiloxane (3 × 5 mL) until the washings were nearly colorless, and recrystallized from OEt_2 yielding 2.41 g (84%) of a lustrous black solid. ^2H NMR (46 MHz, pentane, 25 °C): δ 8.0 ppm (s, $\Delta\nu_{1/2} = 14$ Hz, $C(CD_3)_2CH_3$). μ_{eff} (300 MHz, 25 °C, C_6D_6): 2.2 μ_B. FTIR (heptane, KBr) $\nu_{CO} = 1797$ cm^{-1} ($^{13}C\equiv O$), $\nu_{CO} = 1840$ cm^{-1} ($^{12}C\equiv O$), in heptane. Anal. Calcd for $C_{37}H_{36}D_{18}N_3OMo$: C, 66.24; H, 8.11; N, 6.26. Found: C, 65.85; H, 8.44; N, 6.19.

6. Synthesis of 1-^{13}COC(O)^{t}Bu. A 1% sodium amalgam (852 mg of Na in 85 g of Hg, ca. 5.5 equiv) was prepared in a 250 mL round bottom flask. THF (100 mL) was added and the mixture was stirred vigorously. Solid black **1**-^{13}**CO** (4.346 g, 6.47 mmol) was added in one portion at 25 °C. After 2 h the reaction mixture turned a bright orange color and was filtered through Celite and dried in vacuo. The resulting residue was extracted into OEt_2 (100 mL) and cooled to −35 °C. Pivaloyl chloride (780 mg, 6.47 mmol) was added at once to the chilled solution, which was subsequently allowed to warm to 25 °C and stirred for 16 h. Removal of volatiles in vacuo yielded a solid that was extracted into pentane (50 mL), filtered through Celite to remove salts, and stored at −35 °C, affording 4.03 g (several crops, 82%) of beige, crystalline **1**-^{13}**COC(O)^{t}Bu.** ^1H NMR (300 MHz, C_6D_6, 25 °C): $\delta = 6.67$ (s, 5), 6.09 (s, 4), 2.10 (s, 3), 1.50 (s, 1), 1.22 ppm (s, $C(CH_3)_3$). ^{13}C NMR (125.66 MHz, C_6D_6, 25 °C): $\delta = 217.15$ **1**-^{13}**COC(O)^{t}Bu**, 173.7 **1**-^{13}**COC(O)^{t}Bu**, 150.74 (aryl), 137.38 (aryl), 131.32 (aryl), 130.98 (aryl), 61.55 (6), 38.9 **1**-^{13}**COC(O)C(CH$_3$)$_3$**, 33.84 (1, 2), 27.32 **1**-^{13}**COC(O)C(CH$_3$)$_3$**, 21.88 ppm (3). Anal. Calcd for $C_{42}H_{45}D_{18}MoN_3O_2$: C, 66.73; H, 8.40; N, 5.56. Found: C, 66.64; H, 8.24; N, 5.79.

7. Synthesis of 1-^{13}CH. Solid sodium metal (353 mg, 15.35 mmol) was added to a 50 mL round-bottom flask and smeared along the walls so as to expose a large amount of clean metal surface. THF (25 mL) was then added to the flask, followed by 5 min of vigorous stirring at 25 °C. Solid beige **1**-^{13}**COC(O)^{t}Bu** (2.01 g, 2.66 mmol) was then added at once and the reaction mixture was stirred vigorously for 3 h, gradually turning dark orange. The volatiles were removed in vacuo and pentane (40 mL) was added to the resulting residue to extract the soluble products. This dark orange solution was filtered through Celite, concentrated to 10 mL, and quenched with acetonitrile (2.4 g, 61.5 mmol), which was added to the cold solution (chilled naturally by solvent evaporation). The mixture was allowed to warm gradually to 25 °C, followed by complete solvent removal in vacuo. A light orange solid remained and was collected on a sintered glass frit and washed thoroughly with acetonitrile until the washings were nearly colorless (4 × 5 mL). The insoluble beige powder that remained on the frit was recrystallized from OEt_2, affording 1.13 g (53%) of analytically pure **1**-^{13}**CH**. ^1H NMR (300 MHz, C_6D_6, 25 °C): $\delta = 6.64$ (s, 5), 6.00 (s, 4), 5.66 (d, **1**-^{13}**C*H***), $^1J_{CH} = 157$ Hz), 2.07 (s, 3), 1.49 ppm (s, 1). ^{13}C NMR (125.66 MHz, C_6D_6, 25 °C): $\delta = 287.5$ (**1**-^{13}***C*H**), 150.8 (aryl), 137.4 (aryl), 130.7 (aryl), 128.0 (aryl), 60.0 (6), 34.2 (1, 2), 21.8 ppm (3). Anal. Calcd for $C_{37}H_{37}D_{18}N_3Mo$: C, 67.75; H, 8.45; N, 6.41. Found: C, 67.61; H, 8.29; N, 6.72.

8. Synthesis of (1-^{13}CK)$_2$. In a 20 mL scintillation vial equipped with a stir bar, **1**-^{13}**CH** (764.5 mg, 1.164 mmol) was dissolved in THF (8 mL) and cooled to −78 °C. While stirring, benzylpotassium (151.6 mg, 1.164 mmol) was added at once as an orange solid and reacted quickly on warming. The solution was stirred for 15 min, allowing it to reach room temperature, followed by removal of volatiles in vacuo. The resulting yellow solid was collected on a sintered frit and washed well with pentane to remove any remaining **1**-^{13}**CH**. The powder left behind was spectroscopically pure (**1**-^{13}**CK**)$_2$ (557 mg, 69%). It was recrystallized by stirring in pentane and then adding THF dropwise until the material had just dissolved. Storing such a solution at −35 °C produced crystals which were appropriate for an X-ray diffraction study. ^1H NMR (300 MHz, C_6D_6, 25 °C): $\delta = 6.86$ (s, 4), 6.60 (s, 5), 2.22 (s, 3), 1.48 ppm (s, 1). ^1H NMR (300 MHz, THF-d_8, 25 °C): $\delta = 6.38$ (sh s, 5), 6.25 (v br s, 4), 2.04 (sh s, 13), 1.31 ppm (s br, 1). ^{13}C NMR (125.66 MHz, THF-d_8, 25 °C): $\delta = 502.3$ (br, **1**-^{13}***C***), 489.8 (br, **1**-^{13}***C***), 160 (br, aryl), 135.9 (aryl), 130.1 (aryl), 124.0 (aryl), 58.4 (6), 34.4 (1, 2), 21.8 ppm (3). Anal. Calcd for $C_{37}H_{36}D_{18}N_3KMo$: C, 64.04; H, 7.84; N, 6.05. Found: C, 64.71; H, 7.59; N, 5.85.

9. Synthesis of [K(Kryptofix 222)][1-^{13}C]. (**1**-^{13}**CK**)$_2$ (35.5 mg, 0.0512 mmol) was dissolved in THF (3 mL) to make a yellow solution. Solid white Kryptofix 222 was added to the stirring solution at 25 °C. The solution remained yellow and was dried in vacuo after 10 min. The yellow material was recrystallized from a pentane/THF mixture. ^1H NMR (300 MHz, THF-d_8, 25 °C): $\delta = 6.26$ (s, 5), 5.71 (v br s, 4), 3.58 (m, crypt), 3.53 (m, crypt), 2.53 (m, crypt), 1.92 (s, 3), 1.50 ppm (s, 1). ^{13}C NMR (125.66 MHz, THF-d_8, 25 °C): $\delta = 501$ (s, **1**-^{13}**C**), 157.7 (br, aryl), 135.4 (aryl), 129.5 (aryl), 123.9 (aryl), 71.5 (crypt),

(68) Pangborn, A. B.; Giardello, M. A.; Grubbs, R. H.; Rosen, R. K.; Timmers, F. J. *Organometallics* **1996**, *15*, 1518.
(69) Evans, D. F. *J. Chem. Soc.* **1959**, 2003.
(70) Sur, S. K. *J. Magn. Reson.* **1989**, *82*, 169.
(71) Becke, A. *Phys. Rev. A* **1986**, *34*, 7406.
(72) Perdew, J. P. *Phys. Rev. B* **1986**, *34*, 7406.
(73) Perdew, J. P. *Phys. Rev. B* **1986**, *34*, 8822.

68.8 (crypt), 58.7 (crypt), 57.9 (crypt), 55.2 (6), 35.4 (1, 2), 21.9 ppm (3). Anal. Calcd for $C_{55}H_{72}D_{18}N_5O_6KMo$: C, 61.71; H, 8.47; N, 6.54. Found: C, 61.28; H, 8.21; N, 6.56.

10. Synthesis of (1-^{13}CLi)$_2$. In a 20 mL scintillation vial **1-^{13}CH** (66.8 mg, 0.1019 mmol) was dissolved in benzene (2 mL). To this solution was added *tert*-butyllithium (6.9 mg, 0.107 mmol) in a 2:1 benzene/ether slurry (2 mL). The solution was stirred for 3 h, at which point all volatile material was removed in vacuo. The remaining light tan solid residue was extracted with pentane (8 mL), the extract filtered through Celite, and the filtrate subsequently concentrated to 3 mL, initiating precipitation of a tan solid. The vial was stored at −35 °C for several hours and subsequent decanting of the supernatant afforded 42 mg (62%) of semicrystalline, solvent-free (**1-^{13}CLi**)$_2$ (dimeric formulation assumed). ^{1}H NMR (300 MHz, C_6D_6, 25 °C): δ = 6.69 (s, 4), 6.63 (s, 5), 2.23(s, 3), 1.49 ppm (s, 1). ^{13}C NMR (125.66 MHz, C_6D_6, 25 °C): δ = 470.1 ppm (sh s, **1-^{13}CLi**). Anal. Calcd for $C_{37}H_{36}D_{18}N_3LiMo$: C, 67.15; H, 8.22; N, 6.35. Found: C, 67.65; H, 8.38; N, 6.50.

11. Synthesis of [Na(benzo-12-crown-4)$_2$][1-^{13}CS]. Yellow (**1-^{13}CK**)$_2$ (149 mg mg, 0.2147 mmol) was stirred in a benzene/ether mixture (1:3, 8 mL) and chilled to −35 °C. Solid S_8 (40.5 mg, 1.26 mmol) was then added to the vigorously stirring solution at once. After 2 h the solution was filtered through Celite to remove a brown cakelike residue, dried, and then transferred to a 20 mL scintillation vial containing a 0.4% Na amalgam (13.5 mg of Na in 2.7 g of Hg, 0.576 mmol, 2.7 equiv) in THF (5 mL). The initially orange mixture turned light yellow within 30 min and after 1.5 h was filtered through Celite and dried to a solid. Spectroscopic data for this crude mixture were consistent with clean formation of diamagnetic (**1-^{13}CSNa**)$_2$. ^{1}H NMR (300 MHz, C_6D_6, 25 °C): δ = 6.68 (s, 5), 6.20 (br s, 4), 3.65 (m, THF), 2.19 (s, 3), 1.73 (s, 1), 1.44 ppm (m, THF). ^{13}C NMR (125.66 MHz, C_6D_6, 25 °C): δ = 292.4 (sh s, Mo≡CS), 153.7 (aryl), 135.7 (aryl), 130.0 (aryl), 125.2 (aryl), 61.0.3 (6), 33.9 (1, 2), 21.0 ppm (3). The crude yellow solid was dissolved in a 1:1 ether/benzene solution (6 mL) to which benzo-12-crown-4 (96.3 mg, 0.429 mmol) was added as a solid. A yellow salt precipitated from solution which was collected and recrystallized from a 3:2 pentane/THF (10 mL) mixture to give 139 mg (56%) of crystalline [Na(benzo-12-crown-4)$_2$][**1-CS**]. Microanalysis was obtained for this ion separated salt. Anal. Calcd for $C_{61}H_{68}D_{l8}MoN_3NaOsS$: C, 63.24; H, 7.48; N, 3.63. Found: C, 63.61; H, 7.39; N, 3.60.

12. Synthesis of [K(benzo-15-crown-5)$_2$][1-^{13}CSe]. Yellow (**1-^{13}CK**)$_2$ (190 mg, 0.274 mmol) was dissolved in a 10:1 OEt_2−THF mixture (5 mL) and chilled to −35 °C. Elemental selenium (105 mg, 1.329 mmol) was added at once as a solid and the heterogeneous mixture was allowed to warm to 25 °C. Within 20 min a light flocculent had begun to precipitate from the solution. Stirring was continued for a total of 2 h, after which time the solvent was removed in vacuo. The resulting yellow residue was washed thoroughly with pentane (3 × 5 mL) to remove **1-^{13}CH**, which was a significant reaction byproduct. The resulting yellow solid obtained was dried, then extracted into benzene (7 mL) and filtered through Celite. Lyophilization of the frozen filtrate gave 118 mg (ca. 56%) of spectroscopically pure (**1-^{13}CSeK**)$_2$. The material was recrystallized from a pentane/ether mixture. ^{1}H NMR (300 MHz, C_6D_6, 25 °C): δ = 6.73 (s, 5), 6.17 (v br-s, 4), 2.22 (s, 3), 1.83 ppm (s, 1). ^{13}C NMR (125.66 MHz, C_6D_6, 25 °C): δ = 271.9 (s, **1-^{13}*CS***), 152.7 (aryl), 137.2 (aryl), 130.7 (aryl), 127.2 (aryl), 62.5 (6), 34.9 (1, 2), 22.1 ppm (3). A yellow solution of (**1-CSeK**)$_2$ (17.6 mg, 0.0228 mmol based on Se) in a 4:1 mixture of ether/THF (2.5 mL) was added to a stirring solution of benzo-15-crown-5 (15.3 mg, 0.0570 mmol) in ether (2 mL). After 5 min all volatile material was removed in vacuo and upon addition of ether (2 mL) a yellow solid precipitated. The supernatant was decanted and the solid was washed further with a 1:1 pentane/ether mixture (2 × 4 mL). Subsequent drying afforded 21 mg (ca. 70%) of the ion-separated salt [K(benzo-15-crown-5)$_2$][1-CSe]. Anal. Calcd for $C_{65}H_{76}D_{18}KMoN_3O_{10}Se$: C, 59.62; H, 7.23; N, 3.21. Found: C, 59.71; H, 7.18; N, 3.17.

13. Synthesis of (1-^{13}CTeK)$_2$. Solid (**1-^{13}CK**)$_2$ (141.5 mg, 0.204 mmol based on K) and elemental tellurium (45 mng, 0.353 mmol) were weighed into a 20 mL scintillation vial equipped with a stir bar. A 10:1 ether/THF mixture (5 mL) was added to the vial at −35 °C, and the resulting heterogeneous mixture was stirred vigorously for 14 h at 25 °C. The reaction mixture adopted a yellow-brown color. Volatile material was removed in vacuo and the crude residue was extracted with pentane (20 mL) and filtered through a fine sintered glass frit, affording a yellow-brown filtrate and a yellow solid (somewhat discolored by the excess tellurium powder remaining on the frit). The yellow powder was spectroscopically pure (**1-^{13}CTeK**)$_2$ and the filtrate contained a mixture of both **1-^{13}CH** and (**1-^{13}CTeK**)$_2$ (^{1}H and ^{13}C NMR). Drying the filtrate in vacuo followed by extraction with pentane (5 mL) afforded, on standing at 25 °C, a second crop of yellow (**1-^{13}CTeK**)$_2$. This crop was combined with the main crop and the combined crude solids were extracted into benzene (5 mL) and filtered to remove residual tellurium powder. The yellow benzene filtrate was frozen and lyophilized to a constant weight of 78 mg (ca. 46%) of analytically and spectroscopically pure (**1-^{13}CTeK**)$_2$. This material was recrystallized from a pentane/THF mixture. ^{1}H NMR (300 MHz, C_6D_6, 25 °C): δ = 6.73 (s, 5), 6.16 (v br s, 4), 2.20 (s, 3), 1.84 ppm (s, 1). ^{13}C NMR (125.66 MHz, C_6D_6, 25 °C): δ = 252.6 (s, **1-^{13}CTe**), 152.6 (aryl), 137.2 (aryl), 130.7 (aryl), 127.3 (aryl), 68.2 (6), 34.7 (1, 2), 22.0 ppm (3). Anal. Calcd for $C_{37}H_{36}D_{18}KMoN_3Te$: C, 54.09; H, 6.63; N, 5.11. Found: C, 54.44; H, 6.78; N, 4.99.

14. Synthesis of 1-^{13}CPCl$_2$. A cold solution of PCl_3 (89.1 mg, 0.6493 mmol) in 2 mL of ether was added to a cold, stirring yellow slurry of (**1-^{13}CK**)$_2$ (450.5 mg, 0.6493 mmol) in ether (15 mL). A flocculent solid precipitated and the mixture's color turned to a much darker yellow. Stirring was continued for 1 h, after which time the mixture was filtered through Celite and dried in vacuo. The resulting brown-yellow residue was stirred vigorously in pentane (4 mL), and then allowed to settle at −35 °C for several hours. A yellow solid settled out of the solution and was collected on a sintered glass frit. This solid was washed with pentane until the washings were colorless. This first crop was then passed through the sintered glass frit with ether, leaving behind an insoluble dark brown particulate. The resulting bright yellow filtrate was dried to afford a first pure crop weighing 197 mg. This procedure was repeated with the brownish filtrate to afford a second pure crop of 65 mg, giving an overall yield of 262 mg (ca. 53%). ^{1}H NMR (300 MHz, C_6D_6, 25 °C): δ = 6.64 (s, 5), 5.88 (v br s, 4), 2.04 (s, 3), 1.45ppm (s, 1). ^{13}C NMR (125.66 MHz, C_6D_6, 25 °C): δ = 294.6 (d, **1-^{13}CPCl$_2$**, $^1J_{CP}$ = 144 Hz), 150.1 (aryl), 137.6 (aryl), 130.7 (aryl), 127.7 (aryl), 62.3 (6), 33.7 (1, 2), 21.8 ppm (3). ^{31}P NMR (202.276 MHz, C_6D_6, 25 °C): δ = 120.1 ppm (d, **1-^{13}CPCl$_2$**). Anal. Calcd for $C_{37}H_{36}D_{18}C_{l2}MoP$: C, 58.72; H, 7.19; N, 5.55. Found: C, 58.64; H, 7.18; N, 5.50.

15. Synthesis of [K(benzo-15-crown-5)$_2$][1-^{13}CCH$_2$CH$_2$S]. A homogeneous yellow solution containing 98.6 mg of (**1-^{13}CK**)$_2$ (0.1421 mmol) in ether/THF (15:1, 3.5 mL) was chilled to −35 °C. A prechilled solution of ethylene sulfide (11 mg, 0.183 mmol) in ether (3 mL) was then added dropwise. Stirring was continued for 1 h at 25 °C, after which time the solution was a light peach color. Removal of the reaction volatiles in vacuo gave an oily residue with ^{13}C and ^{1}H NMR data consistent with a major new product (**1-^{13}CCH$_2$CH$_2$SK**)$_x$ along with ca. 30% **1-^{13}CH**. ^{1}H NMR (300 MHz, C_6D_6, 25 °C): δ = 6.65 (s, 5), 6.09 (v br s, 4), 4.30 (br m, SC*H*$_2$CH$_2$C≡Mo), 3.85 (br m, SC*H*$_2$CH$_2$-CMo), 2.13 (s, 3), 1.76 ppm (s, 1). ^{13}C NMR (125.66 MHz, C_6D_6, 25 °C): δ = 304.0 (br, Mo≡*C*CH$_2$CH$_2$S$^-$K$^+$), 151.7 (aryl), 137.3 (aryl), 131.0 (aryl), 61.4 (6), 35.0−34.0 (1, 2, and overlapping methylene carbons), 22.0 ppm (3). Attempts to crystallize (**1-^{13}CCH$_2$CH$_2$SK**)$_x$ from pentane were not successful. However, addition of ca. 2 equiv of benzo-15-crown-5 to the crude product mixture in ether/THF (10:1) effected precipitation of the yellow salt [K(benzo-15-crown-5)$_2$][**1-^{13}CCH$_2$CH$_2$S**]. Decanting the supernatant and subsequent pentane washing of the remaining solid effected removal of the **1-^{13}CH** impurity. Recrystallization from pentane/THF afforded 52 mg of crystalline [K(benzo-15-crown-5)$_2$][**1-CCH$_2$CH$_2$S**]. Anal. Calcd for $C_{67}H_{80}D_{18}N_3$-$KMoO_{10}S$: C, 62.35; H, 7:65; N, 3.26. Found: C, 61.87; H, 7.59; N, 3.25.

16. Solution ^{13}C NMR Data for (1-^{13}CK)$_2$ in THF. A 30 mM solution of (**1-^{13}CK**)$_2$ was prepared by dissolving (**1-^{13}CK**)$_2$ (33.9 mg) and benzyl potassium (9.5 mg) in THF (1.34 mL). The relative concentrations of (**1-^{13}CK**)$_2$ and [K(THF)$_x$][**1-^{13}C**] were determined from ^{13}C NMR integrations of the labeled carbon peaks at δ 501 and

Table 4.

reactant A	reactant B	time	ratio, [**1**-^{13}**C**]$^-$:**1**-^{13}**CH**
[**1**-^{13}**C**]$^-$ (18.5 mg, 0.0267 mmol)	Ph_3CH (6.5 mg, 0.0266 mmol)	20 min	9:1
1-^{13}**CH** (12.4 mg, 0.0189 mmol)	Ph_3CK[a]	36 h	3:17
[**1**-^{13}**C**]$^-$ (16 mg. 0.0231 mmol)	PhC≡CH (7.3 mg, 0.0715 mmol))	upon mixing	complete **1**-^{13}**CH**
[**1**-^{13}**C**]$^-$	toulene (566 mgs)	36 h	complete **1**-^{13}**CH**

[a] Ph_3CH (6.4 mg, 0.0262 mmol) and BzK (3.4 mg, 0.262 mmol).

Table 5. Experimental Spectrum

sample	temp(°C)	δ	$\Delta_{1/2}$ (ppm)	δ	$\Delta_{1/2}$ (ppm)	τ (s)
A	−90	500	2.2	289	3.6	4×10^{-4}
A	−60	498	12	290	17	9×10^{-5}
A	−40	495	30			4×10^{-5}
B	20			309	34	5×10^{-6}
B	0			300	25	1×10^{-5}
C	0			300	25	6×10^{-5}
D	20			292	11	1×10^{-5}

488 ppm. For 2 [K(THF)$_x$][**1**-^{13}**C**] ⇌ (**1**-^{13}**CK**)$_2$, $K_{eq} = [([K][\mathbf{1}\text{-}^{13}\mathbf{C}])_2]/[([K(THF)_x][\mathbf{1}\text{-}^{13}\mathbf{C}])]_2$. K_{eq}(0 °C) = 22.5 M^{-1}, K_{eq}(−10 °C) = 27.3 M^{-1}, K_{eq}(−20 °C) = 31.4 M^{-1}, K_{eq}(−30 °C) = 44.3 M^{-1}, K_{eq}(−40 °C) = 56 M^{-1}, K_{eq}(−50 °C) = 84.5 M^{-1}. The data were then plotted as 1/T vs ln K, to give $\Delta H = -6.7$ kJ/mol and $\Delta S = -23$ J/(mol K). For the fit, $R^2 = 0.99$.

17. T_2 Measurements for 1-^{13}CH and [K(Kryptofix 222)][1-^{13}C]. The T_2 measurements were calculated using the formula $T_2 = (W\pi)^{-1}$, where W is the peak width at half-height. Because of the extremely short values of T_2 obtained, the contribution from field in homogeneities was ignored. **1**-^{13}**CH** (30 mM in THF, 125 MHz): 20 °C, 16 ms; 0 °C, 37 ms; −20 °C, 67 ms. [K(2,2,2-crypt)][**1**-^{13}**C**] (20 mM in THF with 8.6 mM BzK, 125 MHz): 20 °C, 5.8 ms; 0 °C, 7.5 ms; −200 °C, 12 ms; −40 °C, 17 ms.

18. T_1 Measurements. T_1 measurements were performed by centering the transmitter on the peak of interest, measuring the 90° pulse angle and then using the inversion recovery (1800−τ−90°) pulse sequence and fitting the resulting peaks to an exponential curve. **1**-^{13}**COC(O)^{t}Bu** (20 °C, 68 mM in C_6D_6, 125 MHz): 0.97 s. **1**-^{13}**CH** (15 mM in THF, 125 MHz): 20 °C, 0.63 s; 0 °C, 0.47 s; −200 °C, 0.32 s; −40 °C, 0.23 s; −60 °C, 0.14s. [K(2,2,2-crypt)][**1**-^{13}**C**] (14 mM in THF with 6 mM BzK and 5 mM Kryptofix 222, 125 MHz): 20 °C, 0.14 s; −90 °C, 0.04 s.

19. Determination of the pK_a of 1-^{13}CH. For all pK_a determinations, the THF solvent was passed through a short column of activated alumina prior to usage. The compounds were both dissolved in THF and added together. After a given time, the volatiles were removed and the mixture was analyzed in C_6D_6. The results are shown in Table 4.

20. Proton Transfer Kinetics. The following samples were prepared: A, 20 mM in [K(Kryptofix 222)][**1**-^{13}**C**], 7 mM in **1**-^{13}**CH**; B, 11 mM in [K(Kryptofix 222)][**1**-^{13}C], 19 mM in **1**-^{13}**CH**; C, 13 mM in [K(2,2,2-crypt)][**1**-^{13}**C**], 12 mM in **1**-^{13}**CH**; and D, 13 mM in [K(Kryptofix 222)][**1**-^{13}**C**], 12 mM in **1**-^{13}**CH**. For sample A the relative concentrations were determined by low-temperature integrations. For the rest of these spectra these parameters were obtained from the spectral simulation. At 200 and 0 °C the measured values for T_2 were used; for the lower temperature spectra these values were estimated at 0.04 s for the carbide and 0.1 s for the methylidyne.

Acknowledgment. The authors are grateful for support from the National Science Foundation (CHE-9988806) and for fellowships to C.C.C. from the Alfred P. Sloan and the David and Lucile Packard Foundations. C.C.C. also wishes to thank the National Science Board for awarding him the 1998 Alan T. Waterman Award. J.B.G. is grateful for a predoctoral fellowship from the National Science Foundation, J.C.P. appreciated greatly a predoctoral fellowship from the Department of Defense, and T.A.B. benefited from the support of the MIT UROP office. Also deserving of thanks are Dr. Daniel Mindiola for help with X-ray crystallography, Dr. Jeff Simpson for helpful discussions regarding solution NMR spectroscopy, and Professor Klaus Theopold for suggesting the possibility that proton transfer was occurring on the NMR time scale. We are grateful to Professor Joseph Templeton for providing information prior to publication. G.W. wishes to thank the Natural Sciences Engineering Research Council (NSERC) of Canada for research and equipment grants. We also are grateful to Professor Almeria Natansohn (Queen's University) for providing access to the ASX200 spectrometer.

Supporting Information Available: Tables of bond lengths and angles, atomic coordinates and anisotropic thermal parameters for **1-CH**, NMR data, equations used for the simulation of spectra for kinetic studies, and details of the DFT calculations (PDF). This material is available free of charge via the Internet at http://pubs.acs.org.

JA003548E